Hindawi
International Journal of Polymer Science
Volume 2020, Article ID 5705143, 16 pages
https://doi.org/10.1155/2020/5705143

Research Article

Improvement of Water Stability of Sand Admixed with Water-Soluble Organic Polymer

Changqing Qi,[1] **Yuxia Bai**,[1] **Jin Liu**,[1] **Zezhuo Song**,[1] **Debi Prasanna Kanungo**,[2] **Fan Bu**,[1] **Qiongya Wang**,[1] **and Zhaojun Zeng**[1]

[1]*School of Earth Sciences and Engineering, Hohai University, Nanjing 210098, China*
[2]*Council of Scientific and Industrial Research (CSIR)-Central Building Research Institute (CBRI), Roorkee 247667, India*

Correspondence should be addressed to Jin Liu; jinliu920@163.com

Received 24 August 2019; Revised 30 May 2020; Accepted 17 June 2020; Published 13 July 2020

Academic Editor: Zhonghua Peng

Weak water stability of soil is one of the prime causes of soil erosion and slope damage. To understand the improvement on the water stability of sand by a soluble organic polymer (polyurethane, PU), we have conducted a series of water-stability and turbidity tests to evaluate the effects of different polymer content, densities, and immersion times. The mechanism of the improvements is investigated based on scanning electron and digital microscopes. Our results reveal that the polymer can effectively improve the water stability of sand, where the water-stability coefficient enhanced from zero to 100. The turbidity of the water after oscillation was determined, and its value reduced from 84.5 to 10 and kept stable, which further proved the PU improvement on the water stability of sand. The results can be considered as the reference for construction and management of riverbanks and drainage ditches.

1. Introduction

The stability of riverbanks and drainage ditches is important for safety, shipping, and agriculture. Riverbank erosion is a common problem, and it is accelerated by the strong pressure of ship waves and weak water stability of the topsoil [1]. Engineering measures are studied worldwide to alleviate this problem. Such measures are divided into two categories: reducing the influence of ship waves and improving the water stability of topsoil. Many physical structures have been investigated to reduce the slope erosion caused by ship waves, such as soft mattress, slide-resistant pile, and sloping breakwater [2, 3]. When the intensity of ship waves is beyond the engineering design, the slope will be destroyed. In addition, a prolonged immersion in water will make these physical measures ineffective. Improving the water stability of topsoil is hence a viable alternative.

The water stability of soil, defined as resistance against external processes of immersion, rainfall, and runoff, is an important measure of sand resistance against degradation [4–6]. The bases of riverbanks and all kinds of drainage channel slopes are submerged under water for a long time. Long-term immersion of soil in water could cause soil disintegration, which is the cause of soil erosion and bank collapses. In particular, the cohesion of sand is much smaller than that of clay, because of which its water stability is generally considered to be weak. To deal with this situation, much attention has been paid to the improvements of the water stability of soil. At present, adding other types of materials into soil is generally accepted as a good method of soil improvement. Such materials include cement [7–9], fly ash [10, 11], inorganic compound [12–14], organic matter [15–18], and organic polymer. Zhang et al. [8] discussed the strength and stability of fiber-reinforced cemented loess (FRCL), and they found that the mixing of cement and fiber significantly improves the strength and stability. Igwe et al. [13] identified the extent of colloidal stability of the soils and the forms of Fe and Al oxides in the soils contributing to their stability. Hamidpour et al. [17] showed that addition of organic matter increases the water stability of calcareous soil. With respect to the reinforcement effect and the impact on the environment, organic polymers have attracted

increasing attention because of their excellent advantages, such as less incorporation, stable effect, and ecological and environmental protection [19–21]. As a new type of reinforcement material, the cost might be a little higher than that of commonly used reinforcement materials, which may be influenced by the development cost of polymers, using amount, using method, and specific situation of engineering. Song et al. [22] discussed that the cost of polyvinyl acetate was about 30-50 dollars/m^2 for different situations. It was predicted according to the good advantages of organic polymers that the cost would be reduced when they were applied extensively in engineering.

The organic polymers improved the surface properties of soil via ion exchange, hydrogen bond, and absorption; combining with the characteristics of long-chain macromolecules, they enhanced the cohesion between soil grains and reduced the void ratio. Therefore, organic polymers effectively improved the properties of soil. Liu et al. [23] investigated that the polymer-reinforced sand still has good shear behavior after immersion when compared to the purely sand material. Mousavi et al. [24] showed that the soil treatment with a polymer stabilizer resulted in an improvement of the California Bearing Ratio and maximum dry density and a reduction in swelling potential. Tisdall and Oades [25] found that the water stability of microaggregates depends on the persistence of organic binding agents. All these studies demonstrated that the polymer is a good candidate in improving the water stability of soil. The commonly used methods for sand stability testing include wet sieving of sand in a dispersion agent solution [26], water drop destruction [27], and mean weight diameter (MWD) [26, 28]. These methods focus on the disintegration of sand without introducing some strength parameters to evaluate the stability.

In this study, we use a water-soluble organic polymer to test its effect on the water stability of sand. The water-stability tests of the sand at different polymer content, densities, and immersion times were carried out. In addition, the turbidity of the solution after oscillation is used to measure the water stability of sand. The mechanisms of the polymer to sand water stability are studied from scanning electron and digital microscopes.

2. Materials and Methods

2.1. Materials. The sand used in this study is taken from Nanjing, China. The properties of the sand are shown in Table 1. The grain size varies from 0.075 mm to 2 mm, and the content of grains between 0.1 mm and 0.5 mm is more than 50%. The curvature coefficient C_c is 1.13 and the coefficient of uniformity C_u is 2.77. It thus classified as poorly graded sand following the Unified Soil Classification System. After X-ray diffraction results, this sand contains mostly quartz and little feldspar.

A type of water-soluble organic polymer polyurethane (PU) was used as an admixture to sand in this study, which is a light-yellow transparent fluid. It was synthesized in the laboratory, and the basic physical and chemical properties were tested. The specific gravity, viscosity, and density of PU are 1.15, 650-700 MPa·s, and 1.18 g/cm^3, respectively, which could be mixed with water at any content. And it is a neutral substance with a solid content of 88%. The coagulation time is 60-1600 seconds.

2.2. Laboratory Chemical Synthesis of Polyurethane (PU). The constitutional formula of PU used in this study is shown in Figure 1(a), which was synthetized based on five main stages including atmospheric distillation, vacuum distillation, cooling, heating, and cooling, as shown in Figure 1(b). This synthesis method follows Liu [29] and Liu et al. [30].

First, the four crude materials, which include polyoxypropylene glycol (PPG, Chemically Pure, Jining Hongming Chemical Reagent Co., Ltd., Jining, China), polyoxyethylene glycol (PEG, Chemically Pure, Shanghai Ika Biotechnology Co., Ltd., Shanghai, China), polylactic acid glycol (PLAG, Chemically Pure, Shanghai Zhenzhun Biological Technology Co., Ltd., Shanghai, China), and toluene (TL, Chemically Pure, Kaifeng CITIC Industry and Trade Chemical Co., Ltd., Kaifeng, China), were mixed in the reaction still and under air distillation at 135°C. Due to the gradual decrease of toluene content in the reaction system, atmospheric distillation was converted to vacuum distillation. The water and toluene in the reaction system were completely removed by vacuum distillation. The reaction system was cooled to room temperature. N_2 was fed into the reaction system to remove air, and the oil seal was carried out after that. Toluene diisocyanate (TDI, Chemically Pure, Yangzhou Tianda Chemical Co., Ltd., Yangzhou, China) was added to the reaction system, and the system was heated for 2.5 hours at 95°C. After the system was cooled to room temperature, ethyl acetate (EAC, Analytical Reagent, Shandong Haoshun Chemical Co., Ltd., Jinan, China) was added. The system was stirred at room temperature. Sodium dodecyl sulfate (SDS, Analytical Reagent, Langfang Pengcai Fine Chemical Co., Ltd., Langfang, China) was added at last, and the PU was obtained after sufficient stirring.

2.3. Laboratory Testing of Water Stability of Sand Treated with PU. In this test, PU was diluted into a solution of different content, which was mixed with sand to make the PU-sand mixture. The PU-sand mixture was pressed into specimens with 61.8 mm diameter and 20 mm height and at different densities. All the specimens were cured in the environment with 20°C and 30% relative humidity for 48 hours. After that, the specimens were put into a ring-knife with the same size as the specimen. The combination was submerged in water for a period of time, and then the ring-knife was removed. For the specimens where disintegration occurs, the area after disintegration was recorded. The measured and calculated methods for disintegration area follow Liu et al. [31]. The specimens without disintegration were removed from the water to carry out the direct shear tests under 100 kPa, 200 kPa, 300 kPa, and 400 kPa normal pressures based on the American Society for Testing Materials (ASTM) standards (ASTM D3080). The detailed parameters of the specimens are shown in Table 2. The triplicates of the specimens were taken, and their average values were used.

2.4. Water-Stability Coefficient Computation. In order to evaluate the effect of PU on the water stability of sand, the

Table 1: The properties of used sand.

Weight percentage content (%)					Grain size parameter			C_c	C_u	Maximum dry density (g/cm^3)	Minimum dry density (g/cm^3)	Specific density
0.075-0.1 mm	0.1-0.25 mm	0.25-0.5 mm	0.5-1 mm	1-2 mm	D_{60} mm	D_{30} mm	D_{10} mm	1.13	2.77	1.66	1.34	2.65
2.1	31.7	48.9	17.1	0.2	0.36	0.23	0.13					

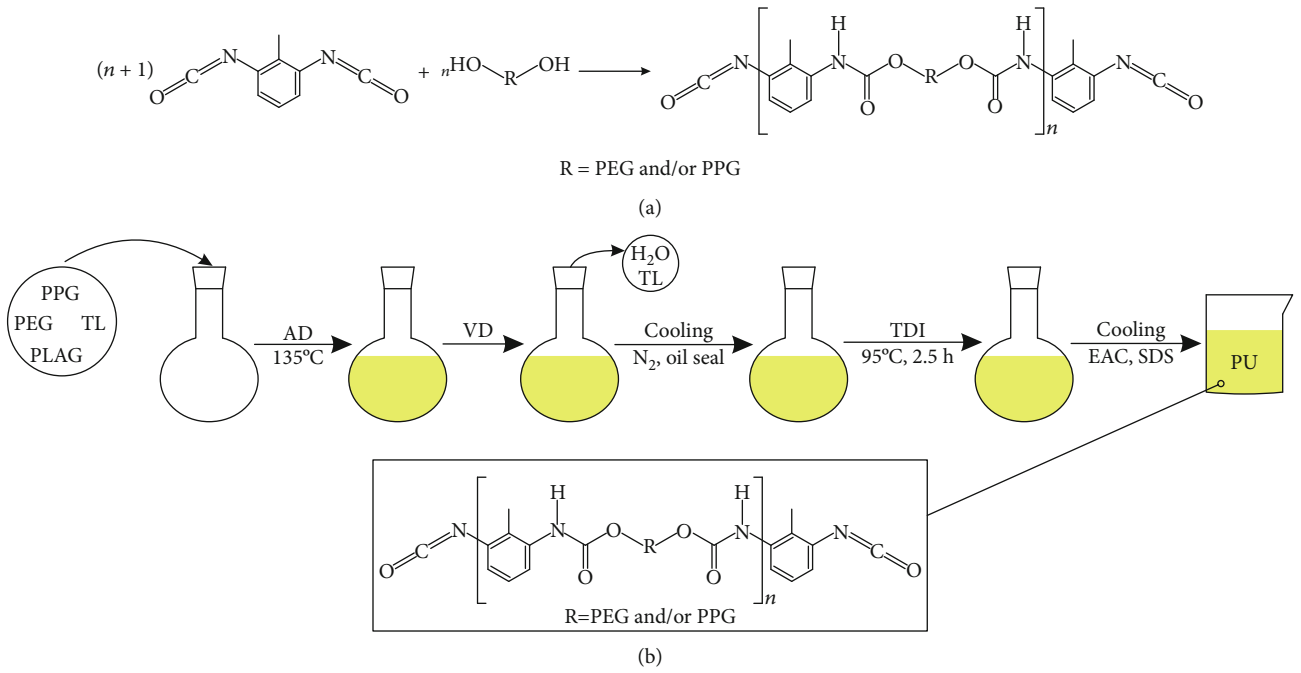

Figure 1: (a) The constitutional formula of polyurethane; (b) the corresponding synthetization diagram.

Table 2: The detailed parameters of the specimens.

Number	Immersion time (h)	Density (g/cm^3)	PU content (%)	Number	Density (g/cm^3)	Immersion time (h)	PU content (%)
S1	24	1.40	0	S11	1.40	24	5
S2	24	1.40	0.1	S12	1.50	24	2
S3	24	1.40	0.2	S13	1.60	24	2
S4	24	1.40	0.3	S14	1.40	0	2
S5	24	1.40	0.4	S15	1.40	1	2
S6	24	1.40	0.5	S16	1.40	3	2
S7	24	1.40	1	S17	1.40	6	2
S8	24	1.40	2	S18	1.40	12	2
S9	24	1.40	3	S19	1.40	48	2
S10	24	1.40	4	S20	1.40	72	2

*PU content is the weight ratio of desired PU to dry sand.

water-stability coefficient was introduced. Based on the basic laws of soil mechanics and the existing studies [32], it could be calculated according to the following formula:

$$K = \frac{S - S_i}{S - S_0} \times 50 + \frac{\tau_1}{\tau_{1\ \max}} \times 12.5 + \frac{\tau_2}{\tau_{2\ \max}} \times 12.5 + \frac{\tau_3}{\tau_{3\ \max}} \times 12.5 + \frac{\tau_4}{\tau_{2\ \max}} \times 12.5, \quad (1)$$

where K (dimensionless) is defined as the water-stability coefficient, and the maximum value of K is 100. S (cm^2) is the disintegration area of the specimen with 0% PU content. S_i (cm^2) is the disintegration area of the specimen with different PU content. S_0 (cm^2) is the initial area of the specimen. In this study, the S_0 is 29.28 cm^2. τ_1, τ_2, τ_3, and τ_4 (kPa) are the shear strength of specimens under 100 kPa, 200 kPa, 300 kPa, and 400 kPa normal pressures, respectively. At the same time, τ_{1max}, τ_{2max}, τ_{3max}, and τ_{4max} (kPa) are the maximum shear

strength of specimens under 100 kPa, 200 kPa, 300 kPa, and 400 kPa normal pressures, respectively. The maximum shear strength was the maximum stress value of the direct shear stress-displacement curve. The application scope of this formula is the PU-sand mixture in this paper.

2.5. Turbidity Measurements of Sand Treated with PU. The preparation process of specimens was the same as that of the water-stability test. The size of the specimens in this test was 39.1 mm diameter and 40 mm height. After curing, the specimen was put in a beaker with an amount of water. The beaker was set on the reciprocating oscillator and oscillated for about 10 minutes. The oscillation frequency was 25 Hz. Three amounts of 25 mL of water were taken from the beaker for turbidity measurements that were made on each aliquot, in nephelometric turbidity units (NTU), using an SGZ-200BS turbidimeter after oscillating. Turbidity measurements were performed every ten minutes, and the total measured time is one hour. The detailed parameters of the specimens are the same with the water-stability test, which is shown in Table 2.

2.6. Microstructure Analysis. In order to analyze the action mechanism of PU in sand, the internal structure of the specimen was obtained through digital microscope and scanning electron microscopy. The digital microscope was used to record the optical images with a magnification of 60x. Also, the scanning electron microscope (SU3500, Hitachi Ltd.) was used to obtain the micrograph with magnifications of 50x and 100x.

3. Results

3.1. Laboratory Testing of Water Stability

3.1.1. Results of the Test. The effect of PU on the water stability of sand was thoroughly studied in the test. According to the experimental methods, the experimental research under different PU content, different densities, and different immersion times was carried out. The results of the test are shown in Tables 3–5, respectively.

3.1.2. Effect of PU Content. Figure 2 displays the disintegration of the specimens with different PU content. As shown in Figure 2 and Table 3, the specimen with 0% PU was severely disintegrated. There were a large number of sand particles distributed in the periphery of the specimen. After measurement, the disintegration area was 102.91 cm^2, which was 2.5 times larger than the initial area. With the increase of PU content, the disintegration of the specimen gradually diminished. The disintegration area of the specimens with 0.1% and 0.2% PU content reduced to 64.99 cm^2 and 49.61 cm^2, respectively. When the PU content was over 0.2%, there was no disintegration, as shown in Figure 2. There were only a few sand particles scattered around the specimens.

The results of direct shear tests of specimens without disintegration are shown in Table 3. Due to disintegration, the specimens with 0%, 0.1%, and 0.2% PU content could not be removed from the water to carry out the direct shear tests, and the shear strengths under different normal pressures of those were considered as zero. The water-stability coefficients of specimens with different PU content were calculated as per Equation (1), and the result is shown in Table 3. Figure 3(a) shows the effect of PU content on the water-stability coefficient. As shown, the water-stability coefficient increased as the PU content increased. When the PU content is 0%, the water-stability coefficient of the specimen is 0, which indicates that the sand has weak water stability. Although the specimens were still unable to remain stable in water, the sand exhibited fixed water stability due to the existence of PU. The water-stability coefficients of the specimens with 0.1% and 0.2% PU content were 25.75 and 36.19, respectively. The water-stability coefficient had a significant increase when the PU content increased from 0.2% to 0.3% and the growth rate was about 121.72%. When the PU content was more than 0.2%, the water-stability coefficient increased slowly. The water-stability coefficient increases from 80.24 to 100, and the growth rate was about 24.63%.

Figure 3(b) shows the typical direct shear stress-displacement curves of the specimens with different PU content under 200 kPa normal pressure. As seen, the shear stress increased with the increase of shear displacement, but the amplitude of increase gradually decreased. Before reaching the peak stress, the slope of each curve gradually increased with an increase in PU content. Compared with the specimens with low PU content, the specimens with high PU content need more shear stress to achieve the same shear displacement, which indicated that the initial stiffness of sand increased gradually with increase of PU content. During the shear process, no obvious peak shear stress was observed and sudden strain softening appeared on the curves of 0.3% to 3% PU content. On the contrary, shear stress tended to be a stable value with shear displacement, which indicated that the specimens presented a significant trend of strain hardening in the later shear period. The two curves of the 4% and the 5% PU content showed obvious peak shear stress and sudden strain softening, which was related to the internal structure and uniformity.

3.1.3. Effect of Density. Considering the properties of used sand and the ease of practical application, the density of 1.40-1.60 g/cm^3 was selected. Disintegration did not occur in this phase. The specimens were in a stable state. There was a small amount of sand particles falling off at the edge of the specimens, which was mainly due to the uneven stress on the edge during specimen preparation.

The water-stability coefficients of specimens with different densities were calculated as per Equation (1), and the results are shown in Table 4. Figure 4(a) shows the effect of density on the water-stability coefficient. The water-stability coefficient increased with the increase in density, as observed from Figure 4(a). The water-stability coefficients of specimens with densities 1.40 g/cm^3, 1.50 g/cm^3, and 1.60 g/cm^3 were 91.23, 94.93, and 100, respectively. In addition, the growth rates between two densities were similar, which are 4.1% and 5.3%, respectively.

Figure 4(b) shows the typical direct shear stress-displacement curves of specimens with different densities

Table 3: The results of the test with different PU content.

Specimen number	Disintegration area S (cm^2)/standard deviation (cm^2)	Shear strength under 100 kPa τ_1 (kPa)/standard deviation (kPa)	Shear strength under 200 kPa τ_2 (kPa)/standard deviation (kPa)	Shear strength under 300 kPa τ_3 (kPa)/standard deviation (kPa)	Shear strength under 400 kPa τ_4 (kPa)/standard deviation (kPa)	Water-stability coefficient K
S1	102.91/3.46	0	0	0	0	0
S2	64.99/1.23	0	0	0	0	25.75
S3	49.61/0.57	0	0	0	0	36.19
S4	29.28/0	49.76/1.79	97.67/2.16	145.59/3.40	193.50/2.91	80.24
S5	29.28/0	51.66/2.71	100.98/2.05	150.29/3.94	199.61/2.34	81.26
S6	29.28/0	53.66/2.16	104.24/3.56	154.82/1.99	205.40/3.70	82.25
S7	29.28/0	59.22/0.14	112.26/3.24	165.29/4.72	218.33/5.69	84.65
S8	29.28/0	81.38/1.98	126.51/2.46	171.64/3.43	216.77/2.21	88.23
S9	29.28/0	89.28/2.74	135.85/3.38	182.42/3.93	228.98/4.34	90.94
S10	29.28/0	121.46/1.87	162.15/1.15	202.84/0.92	243.53/5.36	98.04
S11	29.28/0	124.50/1.87	168.46/1.67	212.42/2.05	256.38/3.22	100.00

Table 4: The results of the test with different density.

Specimen number	Disintegration area S (cm^2)/standard deviation (cm^2)	Shear strength under 100 kPa τ_1 (kPa)/standard deviation (kPa)	Shear strength under 200 kPa τ_2 (kPa)/standard deviation (kPa)	Shear strength under 300 kPa τ_3 (kPa)/standard deviation (kPa)	Shear strength under 400 kPa τ_4 (kPa)/standard deviation (kPa)	Water-stability coefficient K
S8	29.28/0	81.38/2.00	126.51/3.07	171.64/1.78	216.77/5.03	91.23
S12	29.28/0	84.39/2.11	136.89/1.93	191.39/1.08	245.89/4.63	94.93
S13	29.28/0	89.22/1.43	153.22/11.63	217.22/3.76	281.22/3.66	100.00

Table 5: The results of the test with different immersion times.

Specimen number	Disintegration area S (cm^2)/standard deviation (cm^2)	Shear strength under 100 kPa τ_1 (kPa)/standard deviation (kPa)	Shear strength under 200 kPa τ_2 (kPa)/standard deviation (kPa)	Shear strength under 300 kPa τ_3 (kPa)/standard deviation (kPa)	Shear strength under 400 kPa τ_4 (kPa)/standard deviation (kPa)	Water-stability coefficient K
S12	29.28/0	99.74/1.24	156.88/2.44	213.32/1.34	260.76/1.09	100.00
S13	29.28/0	99.03/1.36	155.38/1.44	211.53/2.57	246.14/5.57	98.99
S14	29.28/0	94.50/1.70	141.94/3.49	217.35/1.70	241.84/3.30	97.48
S15	29.28/0	92.73/2.19	135.46/3.13	203.72/4.82	237.04/5.38	95.72
S16	29.28/0	87.54/1.25	133.85/1.36	183.85/2.08	233.76/5.43	93.62
S8	29.28/0	81.38/1.56	126.51/2.22	171.64/4.98	216.77/2.16	90.73
S17	29.28/0	78.73/1.67	120.76/2.35	165.22/4.55	210.39/4.95	89.26
S18	29.28/0	75.83/1.52	117.15/1.39	155.54/4.90	205.52/4.07	87.80

under 200 kPa normal pressure. As shown, the shear stress increased with an increase in shear displacement, but the amplitude of increment gradually decreased. Before reaching the shear peak, the slope of each curve showed no significant difference, which indicated that the density had a little effect on the initial stiffness of the sample. During the shearing process, no obvious peak shear stress and sudden strain softening appeared on the curves of 1.40 g/cm^3 and 1.50 g/cm^3. But the curve of 1.60 g/cm^3 showed obvious peak shear stress and sudden strain softening. This phenomenon was related to an increase in sand suction and the strength of the structure due to density increase. Compared with the low density specimen, the high density specimen appeared brittle, but the brittleness is smaller.

3.1.4. Effect of Immersion Time. The specimens were observed to be stable under different immersion times, which could be ascertained from the value of disintegration area S in Table 5. For the specimens with little immersion times, there were almost no sand particles falling off from their edges. With the increasing immersion time, small amounts of sand particles were observed falling off from the edge of the

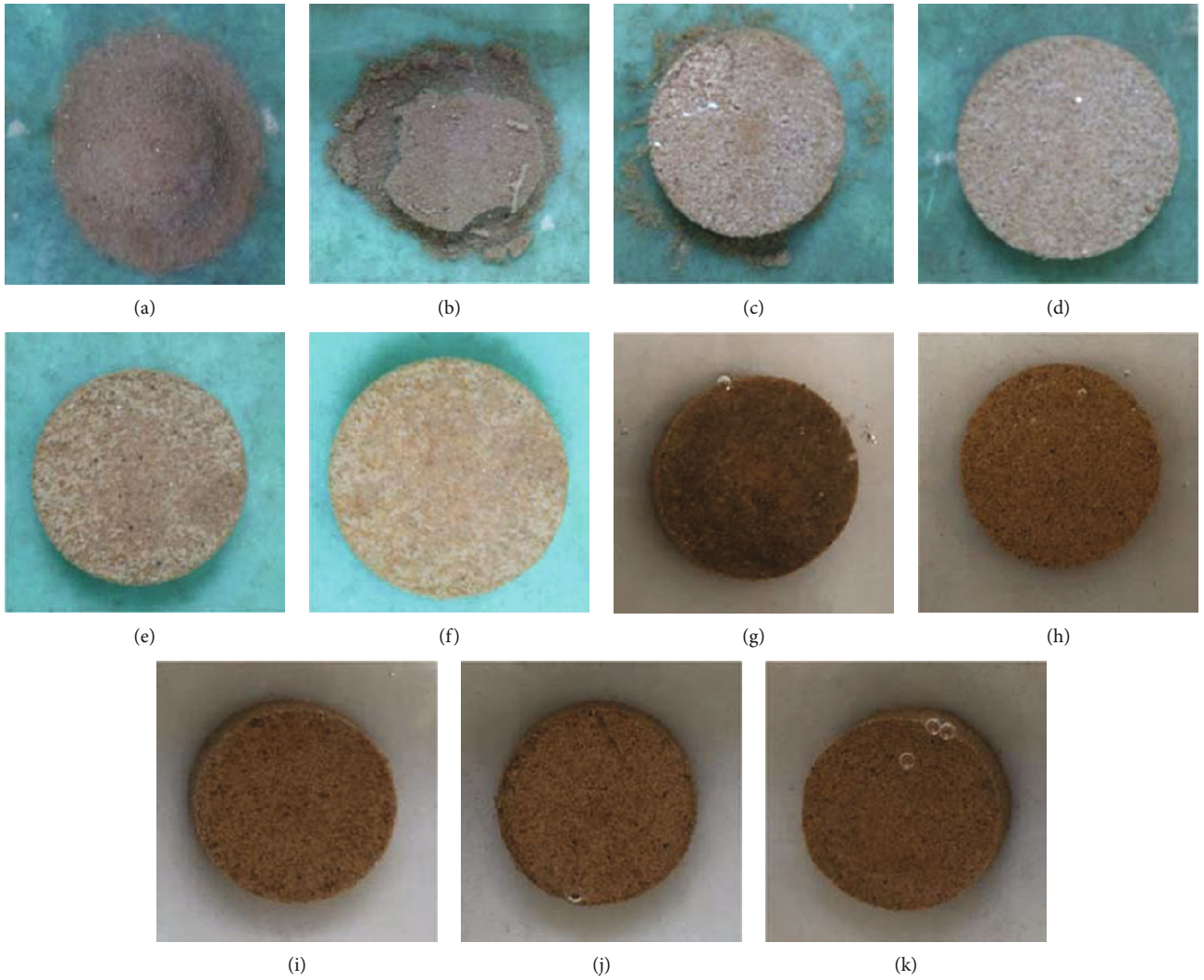

Figure 2: The disintegration of the specimens with different PU content: (a) 0%; (b) 0.1%; (c) 0.2%; (d) 0.3%; (e) 0.4%; (f) 0.5%; (g) 1%; (h) 2%; (i) 3%; (j) 4%; (k) 5%.

specimens. But the specimens remained stable as a whole, and the disintegration did not occur.

The results of direct shear tests of specimens with different immersion times are shown in Table 5. The shear strength under 100 kPa, 200 kPa, 300 kPa, and 400 kPa and the disintegration area were substituted into the Equation (1) to get the water-stability coefficients of specimens with different immersion times. The calculated results are shown in Table 5, and the variation trend is shown in Figure 5(a). As shown, the water-stability coefficient decreased with the increasing immersion time. The water-stability coefficients of specimens with immersion times of 0 h, 1 h, 3 h, 6 h, 12 h, 24 h, 48 h, and 72 h are 100, 98.99, 97.48, 95.72, 93.62, 90.73, 89.26, and 87.80, respectively. The decreasing trend of the curve could be divided into three states: Stage I, Stage II and Stage III. In Stage I, the decreasing trend was slow. In this part, the immersion time was lower than 6 h and the decreasing rate was 1.45%. When the immersion time was between 6 h and 24 h, the variation of the curve entered into Stage II. The decreasing rate of the water-stability coefficient was 2.64%, which was twice compared with Stage I. With the increase of immersion time, the decreasing rate of the water-stability coefficient further slowed down and the curve entered into Stage III. The decreasing rate was 1.62%, which was similar to the decreasing rate in Stage I.

Figure 5(b) shows the typical direct shear stress-displacement curves of specimens with different immersion times under 200 kPa pressure. As observed, the shear stress increased with an increase in shear displacement, but the amplitude of increase decreased with the increasing shear displacement. The shear stress eventually tended to a stable value, which decreased with increasing immersion time. The maximum shear stresses of specimens with immersion times of 0 h, 1 h, 3 h, 6 h, 12 h, 24 h, 48 h, and 72 h were 158.07 kPa, 151.72 kPa, 145.84 kPa, 138.63 kPa, 134.86 kPa, 126.41 kPa, 118.23 kPa, and 111.90 kPa, respectively. During the whole shear process, the shear stress of the specimen with 0 h immersion time was higher than that of the specimens with other immersion times. It can be seen form the shear stress-displacement curves of specimens with different

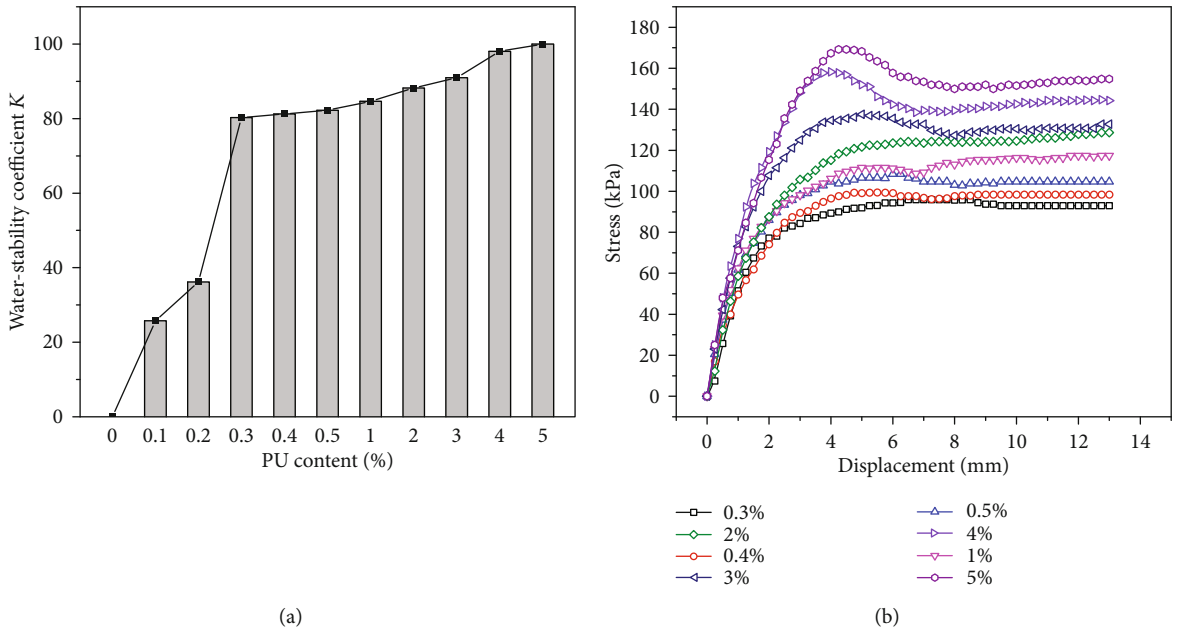

Figure 3: (a) The effect of PU content on the water-stability coefficient; (b) the typical direct shear stress-displacement curves.

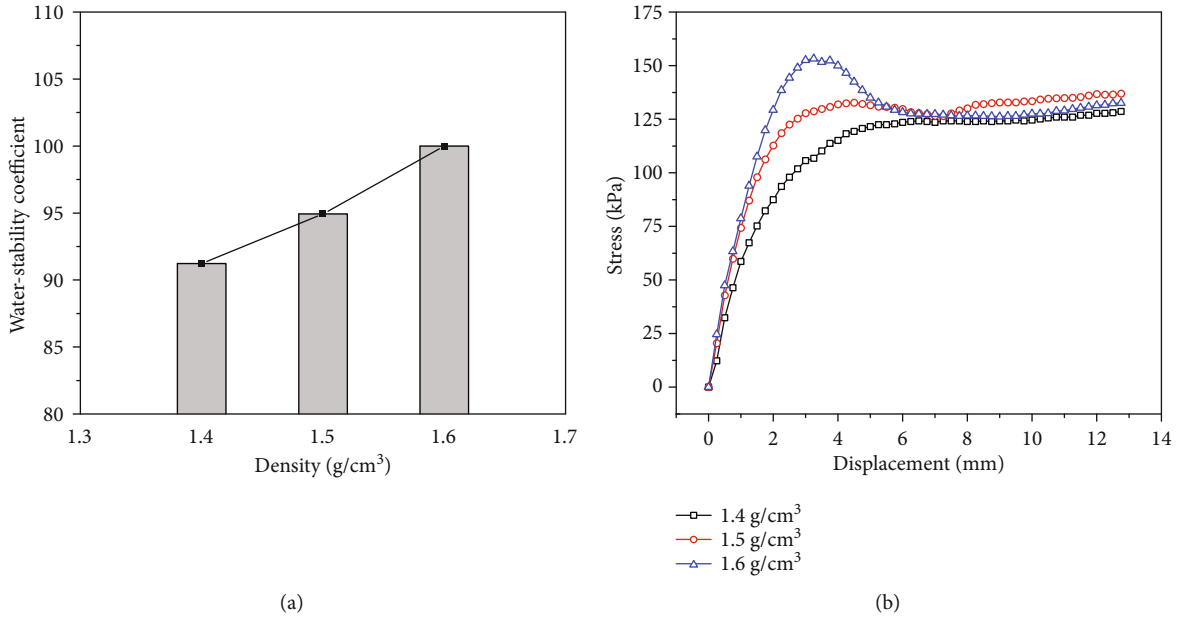

Figure 4: (a) The effect of density on the water-stability coefficient; (b) the typical direct shear stress-displacement curves.

immersion times that the specimen changed from strain hardening to strain softening with the increasing immersion time. When the immersion time was between 0 h and 1 h, no peak shear stress and sudden strain softening appeared on the curves. When the immersion time was more than 1 h, there was an obvious peak shear stress that appeared on the curves. When the specimen was immersed in water, the water gradually entered into the specimen, which reduced the strength and made the specimen soften. But the strain softening kept relatively stable with the increasing immersion time, as shown in Figure 5(b). The strain-softening rates of specimens with 3 h, 6 h, 12 h, 24 h, 48 h, and 72 h were 3.96%, 3.70%, 4.57%, 4.77%, 3.46%, and 3.91%, respectively. It indicated that PU can enhance the antisoftening ability of the specimens.

3.2. Turbidity Measurements of Sand Treated with PU

3.2.1. Results of the Test. The effect of PU on the turbidity of sand was thoroughly studied in this test. According to the experimental methods, the experimental research under different PU content and different immersion times was carried out. In this test, the turbidity of different specimens at 0 min, 10 min, 20 min, 30 min, 40 min, 50 min, and 60 min was

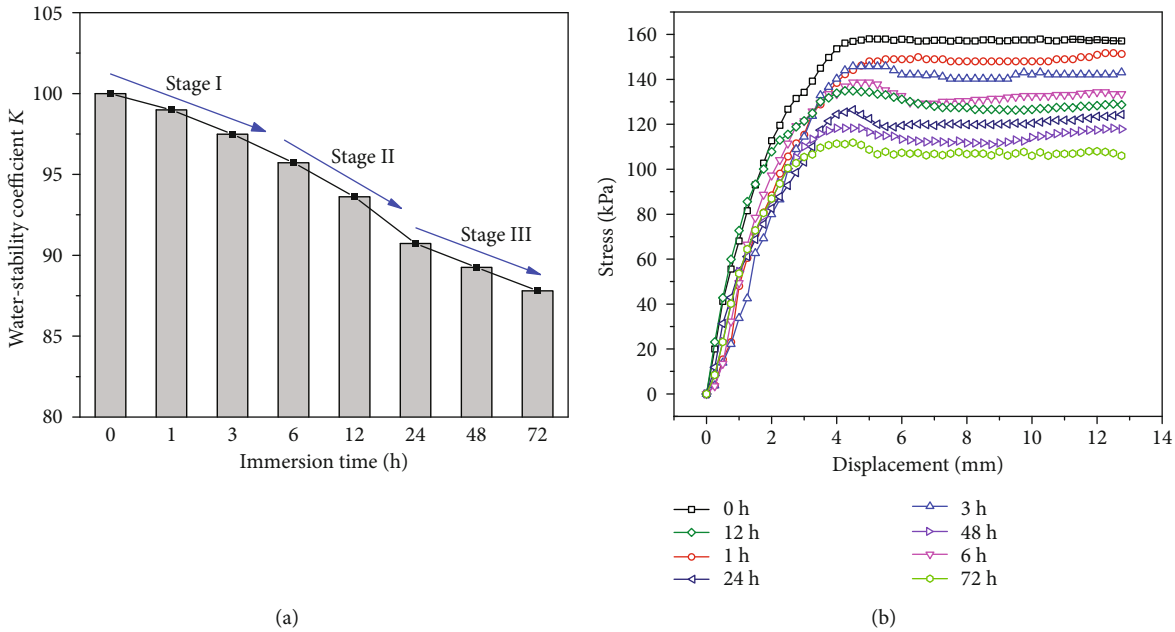

Figure 5: (a) The effect of immersion time on the water-stability coefficient; (b) the typical direct shear stress-displacement curves.

recorded as T_0, T_1, T_2, T_3, T_4, T_5, and T_6. The turbidity of the water used in this test was 0 NTU. The results of these tests are shown in Table 6.

3.2.2. Effect of PU Content. Figure 6 shows the state of the specimens with different PU content after oscillation. As shown in Figure 6(a), the water of the specimen with 0% PU content was too cloudy to see the specimen in the beaker. With the increasing PU content, the water gradually became clear. As shown in Figure 6(e), the water was clear after oscillation when the PU content was 0.4%. Although the water was clear, significant damage occurred to the specimen. All the specimens remained intact when the PU content was over 0.4%, which can be seen in Figures 6(f)–6(k). There were only a few sand particles scattered around the specimens.

Figure 7(a) shows the effect of PU content on the turbidity. As shown, the initial turbidity (T_0) decreased first and then remained unchanged with an increase in PU content. When the PU content was 0%, the initial turbidity (T_0) was 84.5 NTU, which was the maximum turbidity in the whole test program. The initial turbidity (T_0) of the specimens with 0.1%, 0.2%, and 0.3% was 74.9 NTU, 65.3 NTU and 45.8 NTU, respectively. The initial turbidity (T_0) had a significant decrease when the PU content increased from 0.3% to 0.4% and the decreasing rate was about 76.2%. When the PU content was more than 0.3%, the initial turbidity (T_0) kept stable and the domain of Walker was 7.5 NTU to 10.9 NTU. The middle turbidity (T_3) had the same trend with the initial turbidity (T_0). The middle turbidity (T_3) decreased when the PU content was below 0.3% and then remained unchanged with an increase in PU content. The final turbidity (T_6) kept stable except for that of the specimen with 0% PU content. The final turbidity (T_6) of the specimen with 0% PU content was 11.8 NTU, which was large compared with others.

Figure 7(b) shows the relationship between the turbidity and the time. When the PU content was 0%, 0.1%, and 0.2%, the turbidity decreased with an increase in time, and the curves could be divided into three stages based on the decreasing rate. In Stage I, the turbidity decreased quickly with an increase in time. The average decreasing rate was 1.93 NTU/min. In Stage II, the decreasing rate (1.36 NTU/-min) was smaller than that in Stage I. In Stage III, the decreasing rate further decreased, which was 0.24 NTU/min. When the PU content was 0.3%, the turbidity decreased with an increase in time, and the curves could also be divided into three stages based on the decreasing rate. But the turning point was different from the curves of 0%, 0.1%, and 0.2% PU content. For the other seven PU content, the curves remained relatively stable around 8 NTU.

3.2.3. Effect of Density. Figure 8 shows the state of the specimens with different densities after oscillation. As shown, the water of specimens with different densities was clear after oscillation. All the specimens remained intact regardless of density. There were only a few sand particles scattered around the specimens.

Figure 9 shows the effect of density on the turbidity. It showed the results of the test and proved the results of Figure 8 in another way. The initial turbidity (T_0) of the specimens with 1.40 g/cm^3, 1.50 g/cm^3, and 1.60 g/cm^3 densities was near 7.7 NTU, which were 7.5 NTU, 7.8 NTU and 7.8 NTU, respectively. The middle turbidity (T_3) had the same trend with the initial turbidity (T_0). The middle turbidity (T_3) kept stable when the density changed from 1.40 g/cm^3 to 1.60 g/cm^3. The final turbidity (T_6) kept stable, which was 7.9 NTU, 7.2 NTU, and 6.2 NTU for different densities, respectively. But it had a certain downward trend. From the final result, the turbidity of the specimen tended to decrease with an increase in density.

Table 6: The results of turbidity measurements.

Number	Immersion time (h)	Density (g/cm^3)	PU content (%)	T_0 (NTU)/standard deviation (NTU)	T_6 (NTU)/standard deviation (NTU)	Number	Immersion time (h)	Density (g/cm^3)	PU content (%)	T_0 (NTU)/standard deviation (NTU)	T_6 (NTU)/standard deviation (NTU)
S1	24	1.40	0	84.5/1.61	11.8/0.36	S11	24	1.40	5	8.0/0.27	8.3/0.25
S2	24	1.40	0.1	74.9/2.49	9.0/0.44	S12	24	1.50	2	7.8/0.34	7.2/0.17
S3	24	1.40	0.2	65.3/2.35	8.0/0.08	S13	24	1.60	2	7.8/0.36	6.2/0.29
S4	24	1.40	0.3	45.8/2.53	8.3/0.98	S14	0	1.40	2	7.2/0.36	6.8/0.24
S5	24	1.40	0.4	10.9/0.30	8.1/0.29	S15	1	1.40	2	7.4/0.14	6.8/0.22
S6	24	1.40	0.5	8.3/0.38	8.4/0.27	S16	3	1.40	2	7.8/0.03	6.9/0.08
S7	24	1.40	1	8.2/0.39	8.3/0.38	S17	6	1.40	2	7.8/0.28	7.2/0.10
S8	24	1.40	2	7.5/0.31	7.9/0.30	S18	12	1.40	2	7.1/0.23	6.5/0.22
S9	24	1.40	3	8.1/0.27	8.4/0.11	S19	48	1.40	2	7.6/0.20	7.9/0.26
S10	24	1.40	4	7.8/0.14	8.2/0.18	S20	72	1.40	2	7.5/0.19	7.1/0.14

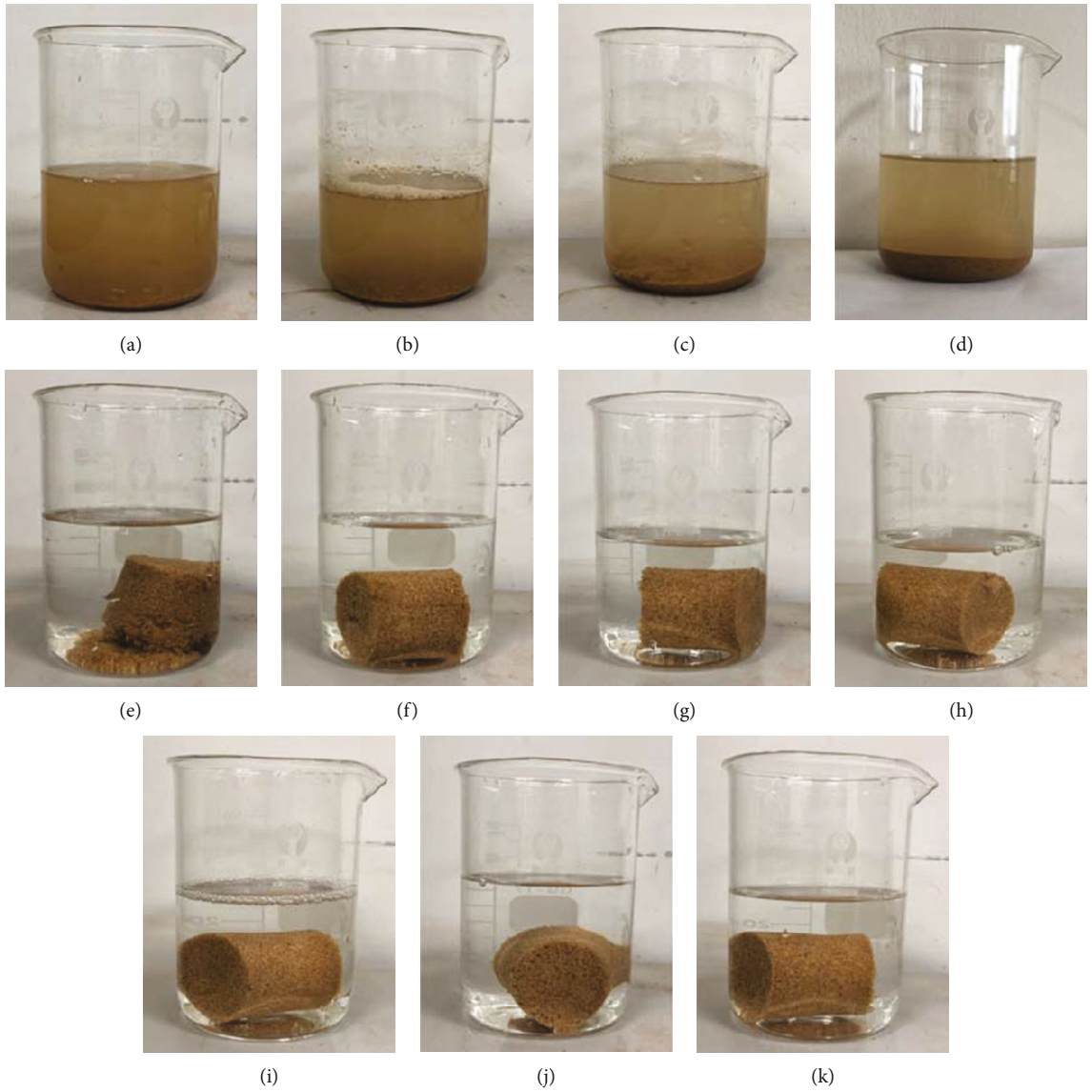

Figure 6: The state of the specimens with different PU content after oscillating: (a) 0%; (b) 0.1%; (c) 0.2%; (d) 0.3%; (e) 0.4%; (f) 0.5%; (g) 1%; (h) 2%; (i) 3%; (j) 4%; (k) 5%.

3.2.4. Effect of Immersion Time. Figure 10 shows the state of the specimens with different immersion times after oscillation. As shown, the water of specimens with different densities was clear after oscillation. Obvious turbidity could not be observed with the naked eye. All the specimens remained intact regardless of density. For the specimens with little immersion time, there was almost no sand particle falling off from their edges. With the immersion time increasing, a small amount of sand particles fell off from the edge of the specimens.

Figure 11 shows the effect of immersion time on the turbidity. The initial turbidity (T_0) kept stable with the immersion time changing from 0 h to 72 h. These values for different immersion times were 7.2 NTU, 7.4 NTU, 7.8 NTU, 7.6 NTU, 7.8 NTU, 7.5 NTU, 7.6 NTU, and 7.5 NTU, respectively. The float range of the middle turbidity (T_3) was relatively large compared with the initial turbidity (T_0). The minimum value appeared, which was 6.5 NTU, when the immersion time was 3 h. The maximum value appeared, which was 8.0 NTU, when the immersion time was 24 h or 72 h. The other middle turbidity (T_3) was within this range. The final turbidity (T_6) had a little float range compared with the middle turbidity (T_3). It varied a small range of between 6.9 NTU and 7.9 NTU.

4. Discussion

The polyurethane used in this study contains an enormous amount of isocyanate groups (-NCO), which could react with water rapidly. Figure 12 shows the detailed process of the reaction of polyurethane with water. As shown in Figure 12, two main reactions occurred when polyurethane was mixed with water. A white emulsion dispersion system was formed, which was mainly composed of polyurea. Due

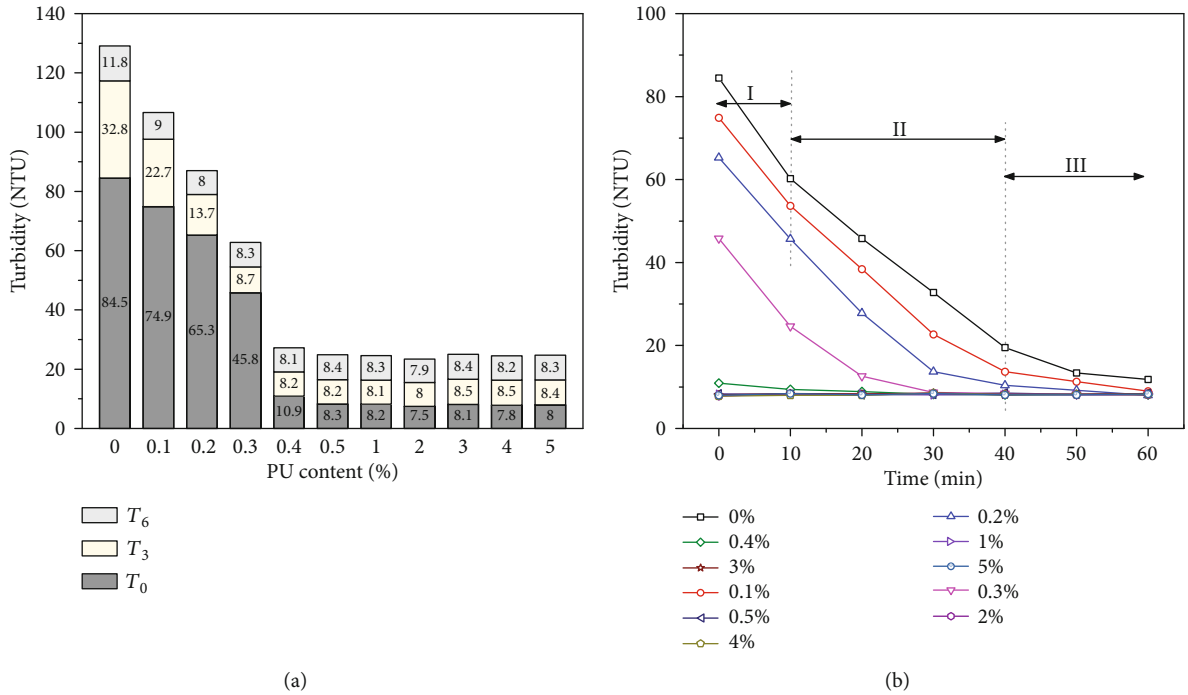

Figure 7: (a) The effect of PU content on the turbidity; (b) the relationship between the turbidity and the time.

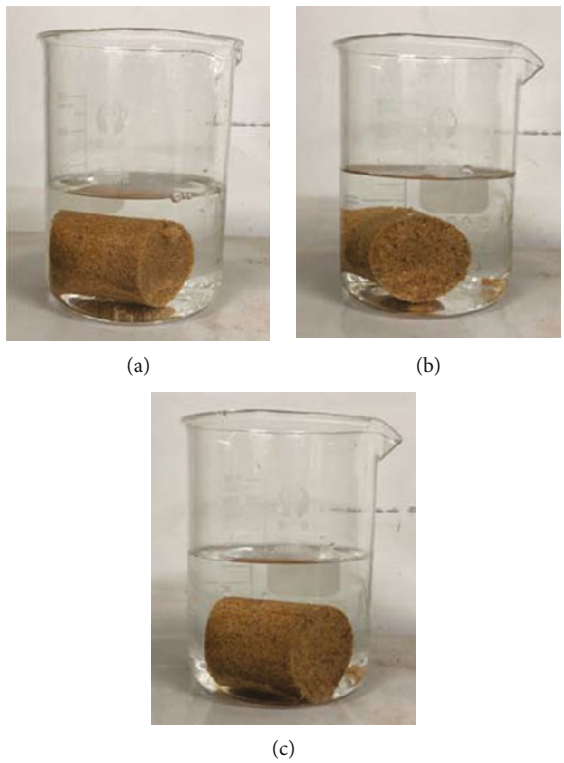

Figure 8: The state of the specimens with different PU content after oscillating: (a) 1.40 g/cm^3; (b) 1.50 g/cm^3; (c) 1.60 g/cm^3.

to the existence of SDS in polyurethane, polyurea could be uniformly dispersed in water, which made the emulsion dispersion system stable for a certain time.

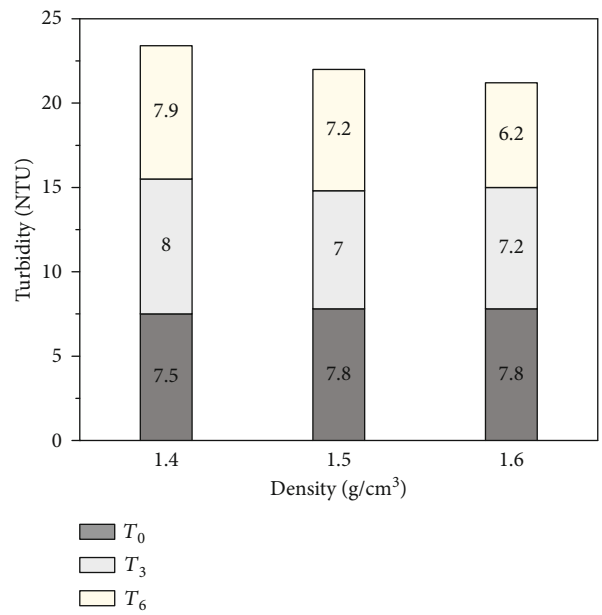

Figure 9: The effect of density on the turbidity.

When the PU was mixed with the water and sand, the polyurea could wrap the sand particles, fill the voids between the sand particles, and connect adjacent sand particles. More specifically, a part of the polyurea could encapsulate the sand particles and form a membrane on the surface of the sand particles. The other part of the polyurea could aggregate between the sand particles and fill a part of the voids. There were a lot of connections between the two parts. By taking the sand particles as the base points and the membranes as

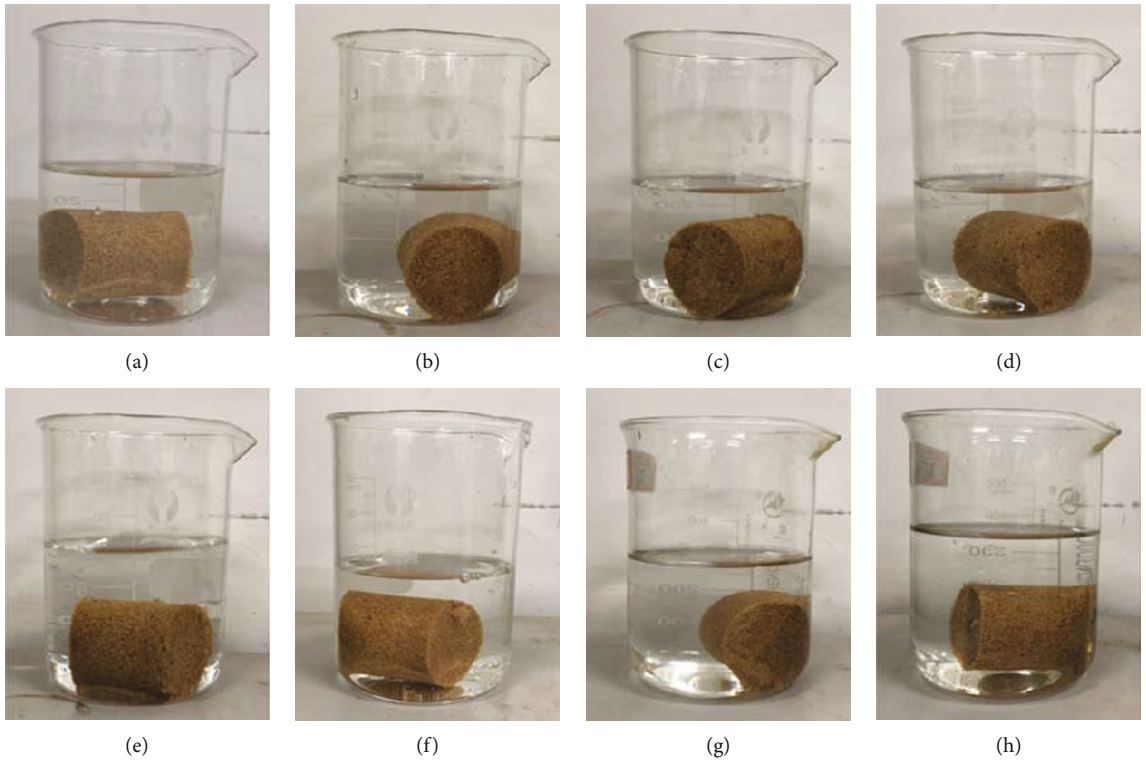

Figure 10: The state of the specimens with different immersion times after oscillating: (a) 0 h; (b) 1 h; (c) 3 h; (d) 6 h; (e) 12 h; (f) 24 h; (g) 48 h; (h) 72 h.

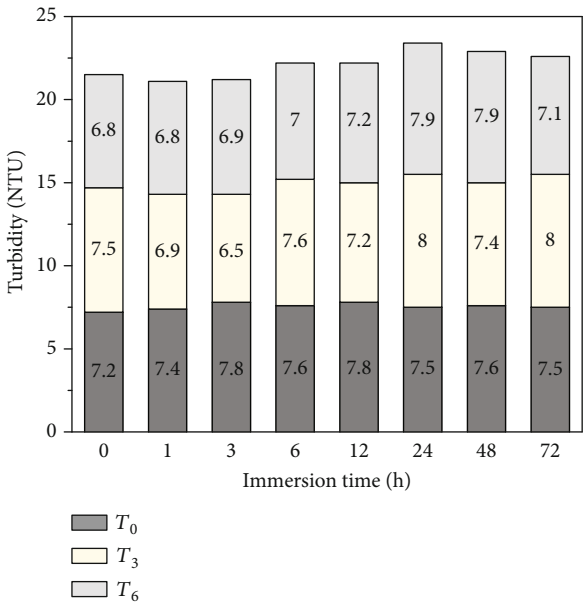

Figure 11: The effect of immersion time on the turbidity.

the interconnecting strands, a complex framework was constructed and then formed into a honeycomb and space network structure, performing a good linking role. Figure 13 shows the scanning electron microscope (SEM) images of the PU-sand mixture. It can be observed from Figures 13(a) and 13(b) that a membrane was closely interfaced on the surface of the sand particles, and it was not easy to separate the membrane from the sand particles. Polyurea aggregated continuously between the sand particles. Finally, it occupied a part of the voids (Figure 13(a)) and connected the adjacent sand particles, thus forming a network structure (Figures 13(c) and 13(d)). Figure 13 also suggests that the sand treated with higher PU content exhibited more a dense and stable structure.

In general, the cohesion of sand is very small compared to clay, which could be neglected in most cases. Figure 14 shows the interaction between the sand particles and water. In the absence of water, the sand particles were arranged loosely and irregularly (Figure 14(a)). When sand was mixed with a small amount of water, water entered the voids between the sand particles. The contact area between the sand particles and water was small compared to the surface area of the sand particles. The surface tension of water connected the sand particles into a whole (Figure 14(b)). When the sand was immersed in water, the voids between the sand particles were completely filled with water. At this time, the expansion pressure of water was greater than the surface tension. The bonding of the sand particles, which lost their interaction with each other, became a loose individual (Figure 14(c)). In this case, the small particles in the sand were suspended in water making the water turbid, when the sand was subjected to external forces (agitation, vibration, impact, etc.).

Figure 15 shows the interaction between the sand particles, PU-formed membrane, and water. When the sand was mixed with PU, PU could form a stable network structure in sand, which could connect the sand particles into a whole

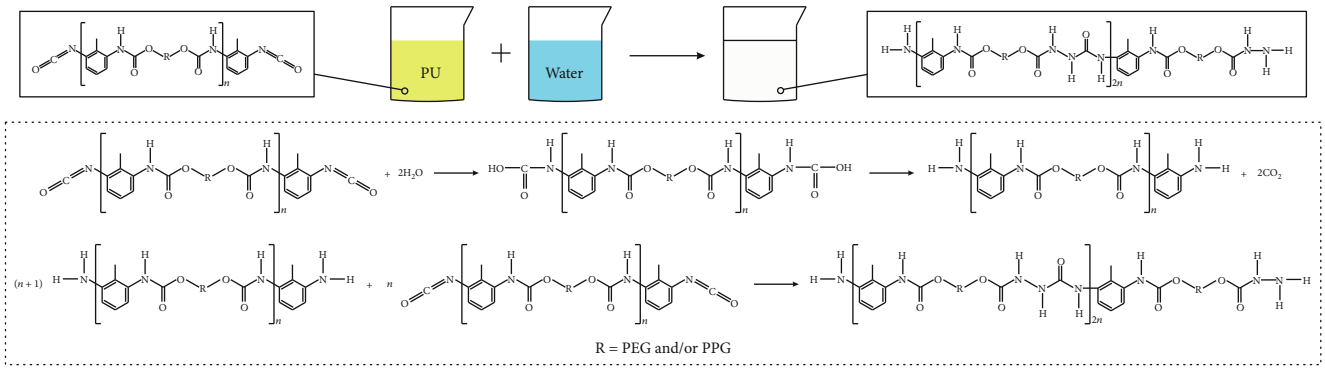

Figure 12: The process of the reaction of polyurethane with water.

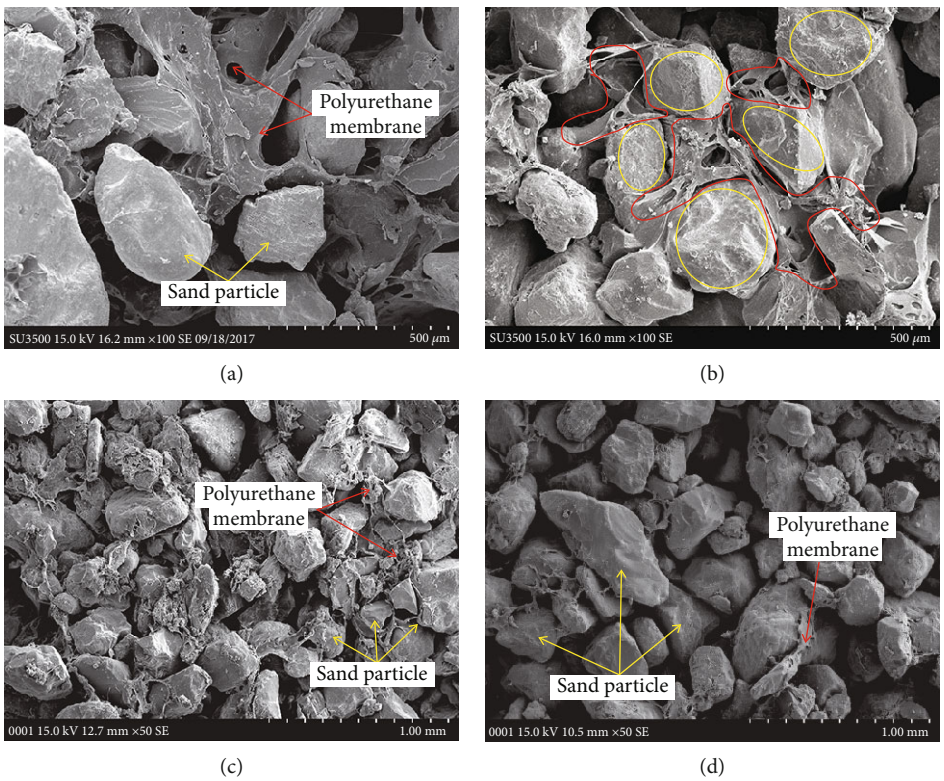

Figure 13: The scanning electron microscope images of the PU-sand mixture: (a) with 4% PU at 100x magnification; (b) with 2% PU at 100x magnification; (c) with 2% PU at 50x magnification; (d) with 1% PU at 50x magnification.

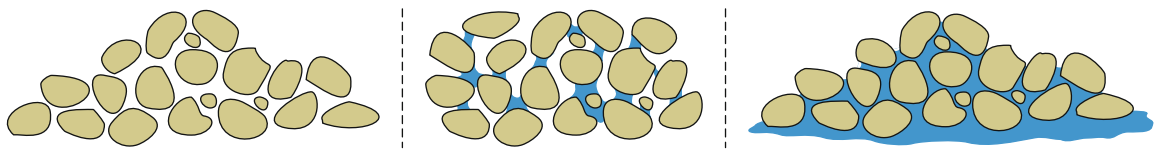

Figure 14: The interaction between sand particles and water: (a) dry sand; (b) sand with small amount of water; (c) sand immersed in water.

(Figure 15(b)). Water could penetrate into the sand particles through infiltration, when the PU-sand mixture was immersed in water. However, the sand could not disintegrate because the tension of the PU-formed membrane was stronger than the expansion pressure of water. The membrane could absorb a certain amount of water, which could further reduce the expansion pressure of water. Figure 16 shows the digital microscope image. As shown in Figure 16, the mixture still retained more water for a period of time after its removal from the water. The PU-sand mixture could remain stable

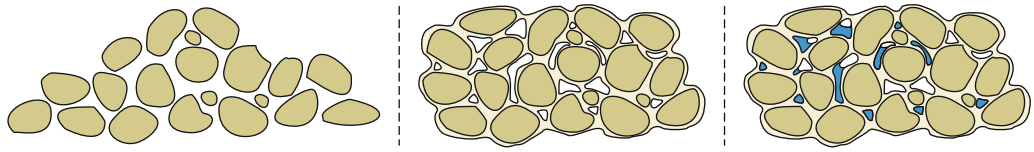

Figure 15: The interaction between sand particles, PU membrane, and water: (a) dry sand; (b) sand mixed with PU; (c) PU-sand mixture immersed in water.

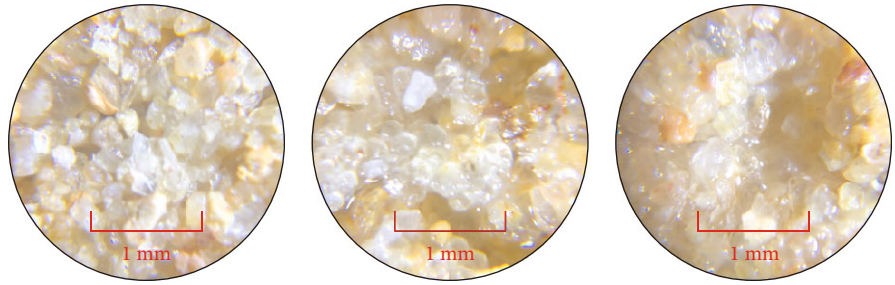

Figure 16: The digital microscope image of PU-sand mixture: (a) without immersion; (b) 0 h after removing from water; (c) 12 h after removing from water.

when the sand was subjected to external forces (agitation, vibration, impact, etc.), which prevented the water from becoming turbid.

Of course, the above situation happened when the PU content was high. In the case of low PU content, the expansion pressure of water in the PU-sand mixture exceeded the strength of the PU-formed membrane, which could result in the disintegration of the PU-sand mixture, when the PU-sand mixture was immersed in water. With the increase in PU content, the mixture did not disintegrate during immersion. But when the content of PU was not enough, some PU-formed membrane could be destroyed under the action of external forces (agitation, vibration, impact, etc.). A large amount of water could enter the PU-sand mixture, causing the expansion pressure of water to exceed the strength of the membrane, resulting in the destruction of the PU-sand mixture and the turbidity of the water.

With the increase in density, the volume of voids in sand decreased and the water stability of sand increased. The two reasons could be summarized as follows. On the one hand, the decrease of the void volume reduced the space for water storage, which leads to the decrease of water expansion pressure. On the other hand, the decrease of the void volume shortened the distance between the sand particles, which leads to the difficulty in sand disintegration. The water stability of sand was improved by both reasons. With the increase in immersion time, the time of water infiltration increased correspondingly. A certain amount of water entering the sandy soil increased the expansion pressure of water, which led to the weakening of the water stability of the sand. However, the volume of the voids in the sand was limited. Density could not be increased indefinitely. And water could not infinitely enter the sand. Therefore, the influence of density and immersion time on the water stability of sand was limited.

Compared with the traditional inorganic sand improvement materials (cement, lime, etc.), inorganic materials have a serious impact on the ecological environment. The soil lost the ability of vegetation growth, which led to the increase of soil pH value in the process used. The natural degradation products of PU-improved soil were nitrogen, carbon dioxide, and water, which had little impact on the ecological environment. After the improvement, the water stability of the soil had been significantly improved, which could promote the stability of the riverbanks and drainage ditches. At present, the research on PU is more concentrated in indoor tests and less involved in the actual project. In the future research, the practical application of PU is the focus of the research.

5. Conclusions

In this paper, the water stability of the sand reinforced with a kind of water-soluble organic polymer (polyurethane, PU) was studied at different conditions. In addition, the turbidity of the water after shaking was also used to evaluate the water stability of the soil. At last, the mechanism of action of the water-soluble organic polymer was discussed based on the interpretations from scanning electron microscopy and digital microscope images. Based on the results obtained, the following conclusions can be drawn:

(1) Polyurethane can effectively improve the water stability of sand. With the increase in PU content, the water-stability coefficient of sand increases from zero to 100. When the content of PU is higher than 0.2%, the sand will not disintegrate in static water. With the increase in density, the water stability of sand increases marginally (the value of K enhanced from 91.23 to 100). The water stability of sand decreases

slightly with the increasing immersion time (the value of K reduced from 100 to 87.80). The water stability of sand remains at a higher level after long immersion

(2) The turbidity of the water after oscillation also proves that the PU could improve the water stability of sand. With the increase in PU content, turbidity decreases first (mainly from 84.5 to 10) and then keeps stable. When the PU content was below 0.4%, the turbidity decreased towards zero with the increase in time. For other PU contents, the curves remained relatively stable around 8 NTU. Density and immersion time have little effects on turbidity, which changes from 6 to 8 NTU

(3) The mechanism of PU in holding the loose sand into a whole in the PU-sand mixture can be explained by the formation of a membrane and a space network structure formed by the membrane. The membrane has enough strength to withstand the expansion pressure caused by water during immersion, so that the PU-sand mixture could achieve good water-stability

Data Availability

In order to verify the results of this article, replicate the analysis, and conduct secondary analyses, any reader or researcher who wishes to obtain the research data of this article, please contact the corresponding author via jinliu920@163.com.

Conflicts of Interest

The authors declare that there is no conflict of interests regarding the publication of this paper.

Acknowledgments

This research was financially supported by the National Natural Science Foundation of China (grant number 41877212); Water Conservancy Science and Technology Project of Jiangsu Province, China (grant number 2017010); and Fundamental Research Funds for the Central Universities (Grant No. 2019B17314).

References

[1] D. M. Lawler, "The measurement of river bank erosion and lateral channel change: a review," *Earth Surface Processes and Landforms*, vol. 18, no. 9, pp. 777–821, 1993.

[2] H. W. Liu, J. X. Luo, P. Lin, and R. Liu, "Analytical solution for long-wave reflection by a general breakwater or trench with curvilinear slopes," *Journal of Engineering Mechanics*, vol. 139, no. 2, pp. 229–245, 2013.

[3] J. J. Xie and H. W. Liu, "Analytical study for linear wave transformation by a trapezoidal breakwater or channel," *Ocean Engineering*, vol. 64, pp. 49–59, 2013.

[4] G. N. Fedotov, Y. D. Tret'yakov, G. V. Dobrovol'skii et al., "Water resistance of soil aggregates and gel structures," *Doklady Chemistry*, vol. 411, no. 1, pp. 215–218, 2006.

[5] R. Kodešová, M. Kočárek, V. Kodeš, J. Šimůnek, and J. Kozák, "Impact of soil micromorphological features on water flow and herbicide transport in soils," *Vadose Zone Journal*, vol. 7, no. 2, pp. 798–809, 2008.

[6] G. Jozefaciuk and H. Czachor, "Impact of organic matter, iron oxides, alumina, silica and drying on mechanical and water stability of artificial soil aggregates. Assessment of new method to study water stability," *Geoderma*, vol. 221-222, pp. 1–10, 2014.

[7] Q. Lv, S. Wang, D. Wang, and Z. Wu, "Water stability mechanism of silicification grouted loess," *Bulletin of Engineering Geology and the Environment*, vol. 73, no. 4, pp. 1025–1035, 2014.

[8] J. Zhang, X. Z. Weng, and J. Z. Liu, "Strength and water stability of a fiber-reinforced cemented loess," *Journal of Engineered Fibers and Fabrics*, vol. 13, no. 1, pp. 72–83, 2018.

[9] H. Tang, X. G. Li, M. L. Li, L. Q. Song, Z. J. Wu, and H. X. Xu, "Properties and mechanism of CFBC fly ash-cement based stabilizers for lake sludge," *Journal of Wuhan University of Technology-Materials Science Edition*, vol. 27, no. 4, pp. 750–753, 2012.

[10] Z. Gu, S. Hua, W. Zhao, S. Li, Z. Gao, and H. Shan, "Using alkali-activated cementitious materials to solidify high organic matter content dredged sludge as roadbed material," *Advances in Civil Engineering*, vol. 2018, Article ID 2152949, 10 pages, 2018.

[11] W. Shen, M. Zhou, W. Ma, J. Hu, and Z. Cai, "Investigation on the application of steel slag–fly ash–phosphogypsum solidified material as road base material," *Journal of Hazardous Materials*, vol. 164, no. 1, pp. 99–104, 2009.

[12] B. G. Barthès, E. Kouakoua, M.-C. Larré-Larrouy et al., "Texture and sesquioxide effects on water-stable aggregates and organic matter in some tropical soils," *Geoderma*, vol. 143, no. 1-2, pp. 14–25, 2008.

[13] C. A. Igwe, M. Zarei, and K. Stahr, "Colloidal stability in some tropical soils of southeastern Nigeria as affected by iron and aluminium oxides," *Catena*, vol. 77, no. 3, pp. 232–237, 2009.

[14] M. Spohn and P. M. Schleuss, "Addition of inorganic phosphorus to soil leads to desorption of organic compounds and thus to increased soil respiration," *Soil Biology & Biochemistry*, vol. 130, pp. 220–226, 2019.

[15] D. Saha, S. S. Kukal, and S. Sharma, "Landuse impacts on SOC fractions and aggregate stability in typic ustochrepts of Northwest India," *Plant & Soil*, vol. 339, no. 1-2, pp. 457–470, 2011.

[16] A. R. Dexter and E. A. Czyż, "Soil crumbling during tillage as a function of soil organic matter content," *International Agrophysics*, vol. 25, no. 3, pp. 215–221, 2011.

[17] M. Hamidpour, M. Afyuni, E. Khadivi, A. Zorpas, and V. Inglezakis, "Composted municipal waste effect on chosen properties of calcareous soil," *International Agrophysics*, vol. 26, no. 4, pp. 365–374, 2012.

[18] R. Kodešová, M. Rohošková, and A. Žigová, "Comparison of aggregate stability within six soil profiles under conventional tillage using various laboratory tests," *Biologia*, vol. 64, no. 3, pp. 550–554, 2009.

[19] J. Liu, B. Shi, H. Jiang, H. Huang, G. Wang, and T. Kamai, "Research on the stabilization treatment of clay slope topsoil by organic polymer soil stabilizer," *Engineering Geology*, vol. 117, no. 1-2, pp. 114–120, 2011.

[20] P. Johnston, G. Freischmidt, C. D. Easton et al., "Hydrophobic-hydrophilic surface switching properties of nonchain extended poly(urethane)s for use in agriculture to minimize

soil water evaporation and permit water infiltration," *Journal of Applied Polymer Science*, vol. 134, no. 45, article 44756, 2017.

[21] T. A. Lerma, M. Palencia, and E. M. Combatt, "Soil polymer conditioner based on montmorillonite-poly (acrylic acid) composites," *Journal of Applied Polymer Science*, vol. 135, no. 18, article 46211, 2018.

[22] Z. Song, J. Liu, Y. Bai et al., "Laboratory and field experiments on the effect of vinyl acetate polymer-reinforced soil," *Applied Sciences*, vol. 9, no. 1, pp. 208–222, 2019.

[23] J. Liu, Y. Bai, D. Li et al., "An experimental study on the shear behaviors of polymer-sand composite materials after immersion," *Polymers*, vol. 10, no. 8, pp. 924–938, 2018.

[24] F. Mousavi, E. Abdi, and H. Rahimi, "Effect of polymer stabilizer on swelling potential and CBR of forest road material," *KSCE Journal of Civil Engineering*, vol. 18, no. 7, pp. 2064–2071, 2014.

[25] J. M. Tisdall and J. M. Oades, "Landmark papers: no. 1. Organic matter and water-stable aggregates in soils," *Eurasian Soil Science*, vol. 63, no. 1, pp. 8–21, 2012.

[26] Z. Li, W. Yang, C. Cai, and J. Wang, "Aggregate mechanical stability and relationship with aggregate breakdown under simulated rainfall," *Soil Science*, vol. 178, no. 7, pp. 369–377, 2013.

[27] C. Chenu, Y. Le Bissonnais, and D. Arrouays, "Organic matter influence on clay wettability and soil aggregate stability," *Soil Science Society of America Journal*, vol. 64, no. 4, pp. 1479–1486, 2000.

[28] T. V. Alekseeva, Z. Sokolowska, M. Hajnos, A. O. Alekseev, and P. I. Kalinin, "Water stability of aggregates in subtropical and tropical soils (Georgia and China) and its relationships with the mineralogy and chemical properties," *Eurasian Soil Science*, vol. 42, no. 4, pp. 415–425, 2009.

[29] J. Liu, *Experimental Study on Development and Application of Polymer Soil Stabilizers*, Nanjing University, 2011.

[30] J. Liu, Y. Bai, Z. Song, Y. Lu, W. Qian, and D. Kanungo, "Evaluation of strength properties of sand modified with organic polymers," *Polymer*, vol. 10, no. 3, p. 287, 2018.

[31] J. Liu, Z. Song, Y. Bai et al., "Laboratory tests on effectiveness of environment-friendly organic polymer on physical properties of sand," *International Journal of Polymer Science*, vol. 2018, Article ID 5865247, 11 pages, 2018.

[32] J. Liu, B. Shi, H. Jiang, S. Bae, and H. Huang, "Improvement of water-stability of clay aggregates admixed with aqueous polymer soil stabilizers," *Catena*, vol. 77, no. 3, pp. 175–179, 2009.